

# Nonequilibrium wetting transitions with short range forces

F. de los Santos,<sup>1,2</sup> M. M. Telo da Gama,<sup>2</sup> and M. A. Muñoz<sup>3</sup>

<sup>1</sup>Center for Polymer Studies and Department of Physics, Boston University, Boston, MA 02215 USA

<sup>2</sup>Departamento de Física da Faculdade de Ciências e Centro de Física da Matéria Condensada da Universidade de Lisboa, Avenida Professor Gama Pinto, 2, P-1643-003 Lisboa Codex, Portugal

<sup>3</sup>Departamento de Electromagnetismo y Física de la Materia, Universidad de Granada, 18071 Granada, Spain

We analyze within mean-field theory as well as numerically a KPZ equation that describes nonequilibrium wetting. Both complete and critical wetting transitions were found and characterized in detail. For one-dimensional substrates the critical wetting temperature is depressed by fluctuations. In addition, we have investigated a region in the space of parameters (temperature and chemical potential) where the wet and nonwet phases coexist. Finite-size scaling analysis of the interfacial detaching times indicates that the finite coexistence region survives in the thermodynamic limit. Within this region we have observed (stable or very long-lived) structures related to spatio-temporal intermittency in other systems. In the interfacial representation these structures exhibit perfect triangular (pyramidal) patterns in one (two dimensions), that are characterized by their slope and size distribution.

PACS numbers: 5.10.-a, 64.60.-i, 68.08.Bc

## I. INTRODUCTION

When a bulk phase is placed into contact with a substrate, a layer of a second, coexisting, phase may form if the substrate preferentially adsorbs it. At a wetting transition, the thickness of the layer diverges. Equilibrium wetting has been experimentally observed and theoretically investigated using, among many other techniques, interface displacement models [1, 2, 3]. Within this approach one considers the local height of the interface measured from the substrate,  $h(\mathbf{x})$ , and constructs an effective interface Hamiltonian,  $H(h)$  [4]. In equilibrium situations, one typically has

$$H(h) = \int_0^{\infty} dx \frac{\sigma}{2} (r h)^2 + V(h) \quad (1)$$

where  $\sigma$  is the interfacial tension of the interface (or the interfacial stiffness if the medium is anisotropic) and  $V(h)$  accounts for the interaction between the substrate and the interface.

If all the microscopic interactions are short-ranged, one may take for sufficiently large  $h$  at bulk coexistence [3]

$$V(h) = b(T)e^{-h} + ce^{-2h}; \quad (2)$$

where  $T$  is the temperature,  $b(T)$  vanishes linearly as  $T \rightarrow T_w$ ,  $T_w$  being the wetting temperature, and  $c > 0$  [5]. By minimizing (1) one finds [1, 3] a critical wetting transition at  $b = 0$ , i.e. the interface height (or equivalently, the wetting layer thickness),  $h_i$ , diverges continuously as  $b \rightarrow T \rightarrow T_w \rightarrow b_w = 0$ . Equilibrium critical wetting has been studied for decades and a rich (non-classical) behavior predicted [1, 2].

Wetting transitions may also be driven by the chemical potential difference between the two phases,  $\mu$ . In this case wetting occurs at any temperature above  $T_w$  (i.e. for  $b > b_w$ ) as  $\mu = 0$  is approached from the nonwet phase.

This is always a continuous transition and it is known as complete wetting [1]. A study of complete wetting requires adding a linear term  $\mu h$  to the Hamiltonian (1).

A dynamic model for the growth of wetting layers has been proposed through the Langevin equation [6]

$$\partial_t h(\mathbf{x};t) = \frac{H}{h} + \nabla^2 h + \frac{\partial V}{\partial h} + \zeta; \quad (3)$$

where  $\zeta$  is Gaussian white noise with mean and variance

$$\begin{aligned} \langle h(\mathbf{x};t) \rangle &= 0; \\ \langle h(\mathbf{x};t) h(\mathbf{x}^0;t^0) \rangle &= 2D(t-t^0) \delta(\mathbf{x}-\mathbf{x}^0); \end{aligned} \quad (4)$$

Equation (3) is an Edwards-Wilkinson (EW) growth equation [7, 8] in the presence of an effective interface potential  $V(h)$ . It describes the relaxation of the interfacial height  $h$  towards its equilibrium value, i.e. the value of  $h$  that minimizes  $H$ . Within this context  $\mu$  can be viewed as an external driving force acting on the interface. Recall that in the absence of the wall, the corresponding equilibrium states for  $\mu < 0$  and  $\mu > 0$  are the nonwet and wet phases, respectively, whereas phase coexistence occurs at  $\mu = 0$ .

Equilibrium models, however, are not sufficient to study wetting in Nature, since in a wide range of phenomena (e.g., growth of thin films, spreading of liquids on solids or crystal growth) thermodynamic equilibrium may not hold. Nonequilibrium wetting transitions have been recently studied by Hinrichsen et al. [9] in a lattice (restricted solid-on-solid) model with dynamics that do not obey detailed balance. The continuum nonequilibrium counterpart of this discrete model, is a Kardar-Parisi-Zhang (KPZ) equation in the presence of a bounding potential, whose properties have been analyzed extensively by one of the authors and collaborators [11, 13]. Clearly this is the most natural extension of the EW equilibrium growth model to non-equilibrium situations. In fact, in

the absence of a substrate the KPZ non-linearity,  $(r h)^2$ , is generically the most relevant nonequilibrium perturbation to the equilibrium EW equation [8]. The KPZ nonlinearity is related to lateral growth, and although this mechanism is unlikely to be relevant in simple fluids, it may determine the wetting behavior of systems with anisotropic interactions for which the growth of tilted interfaces depends on their orientation [14]. For instance, it has been shown that crystal growth from atomic beams is described by the KPZ equation [15]. From a theoretical point of view a key and ambitious task is that of developing general criteria to establish whether the KPZ non-linear term should be included in a given interfacial model.

Related works published recently by Muller et al. [16], Giada and Marsili [17], Hinrichsen et al. [18], and ourselves [10], consider similar non-equilibrium models in the presence of various types of walls.

In this paper, we further study the KPZ interfacial equation in the presence of different types of potentials, attractive and repulsive. We focus on the connection of the associated phenomenology with non-equilibrium wetting and depinning transitions. In particular, we will stress that the transitions called "first-order non-equilibrium wetting" in [18] are not wetting transitions but, rather, depinning transitions. Also, we study for the first time the two-dimensional version of this model, and report on new phenomenology.

The remainder of this paper is organized as follows. In the next section we introduce our KPZ-like model. A mean-field picture is provided in section III, and its predictions numerically tested in section IV. The conclusions are summarized in the final section.

## II. THE MODEL

The model under study is defined by the Langevin equation

$$\partial_t h(x;t) = r^2 h + (r h)^2 \frac{\partial V(h)}{\partial h} + \zeta; \quad (5)$$

where  $V(h) = (a+1)h + bh^c + ce^{2h}$ ,  $c > 0$ , obeys (4) and  $a+1 = \mu$  is a chemical potential.

In the absence of the exponential terms (the limiting wall) the interface moves with a nonzero positive (negative) mean velocity for larger (smaller) than a certain critical value  $c_c$ . In one dimension  $c_c$  can be found analytically since both the KPZ and EW equations have the same Gaussian steady-state height distribution [8]. Thus  $c_c = h(rh)^2$ , which for discrete lattices can be approximated by [19]  $c_c = (D)^{-2}$ , being the lattice cutoff. Note that for  $\mu \leq 0$  a nonzero chemical potential is required to balance the force exerted by the nonlinear term on the tilted interfacial regions. For  $\mu = 0$  the model reduces to the equilibrium one and  $c_c = 0$  as usual. For negative values of  $\mu$  the interface is (on average) pushed against the wall, while for positive  $\mu$  it is

pulled away from the wall. Thus the behavior of the system is determined by the sign of  $\mu$  [20]. In this paper we will consider  $\mu < 0$  only (which corresponds to the case studied using microscopic models [18]). Results for positive values of  $\mu$  will be published elsewhere.

It is our purpose to study the effects of a substrate that adsorbs preferentially one of the two phases on the stationary properties of the interface. This is achieved by considering  $b$  to be negative in equation (5).

This same equation, (5), has been recently studied by Giada et al. [17] as a generic nonequilibrium continuum model for interfacial growth. However, their choice of control parameters [17] privileges the role of the noise as the driving force of the nonequilibrium transitions. By contrast, motivated by the role of the chemical potential and temperature in equilibrium wetting, we fix the noise intensity and choose  $a$  and  $b$  as control parameters that are the fields driving critical and complete wetting transitions.

To establish the analogy with equilibrium, let us stress that just like in equilibrium complete wetting, nonequilibrium complete wetting occurs when the attractive potential  $V(h)$  is not capable of binding the interface, at temperatures above the wetting transition temperature,  $b > b_W$ , as the chemical potential approaches that of bulk coexistence,  $\mu = \mu_c$ . At this transition the interface begins to move and  $h$  diverges. On the other hand, the nonequilibrium analogue of critical wetting corresponds to the unbinding of a bound interface at bulk coexistence,  $\mu = \mu_c$ , as  $b \rightarrow b_W$ .

In order to analyze equation (5) it is convenient to perform a Cole-Hopf change of variable  $h(x;t) = \ln n(x;t)$ , leading to

$$\partial_t n = r^2 n \frac{\partial V(n)}{\partial n} + \zeta; \quad (6)$$

with  $V(n) = an^2 + bn^3 + cn^4$ . This describes the interface problem as a diffusion-like equation with multiplicative noise [11, 21]. In this representation, the unbinding from the wall ( $h \rightarrow \infty$ ) corresponds to a transition into an absorbing state  $n \rightarrow 0$ . In the following we will use both languages,  $h$  and  $n$ , indistinctly although the natural description of wetting is in terms of  $h$ . The case  $b > 0$  was studied in [9, 11], while  $b < 0$  is the case studied in [10, 16, 17, 18, 22].

Note that we have made use of Ito calculus, and thus equation (6) should be interpreted in the Ito sense [23]. In general, potentials of the form  $bn^{p+2} = (p+2) + cn^{2p+2} = (2p+2)$  with  $p > 0$  result in equivalent effective Hamiltonians since, when expressed in terms of  $h$ ,  $p$  can be eliminated by redefining the height scale. The case  $p = 2$  (with fixed  $b < 0$ ) has been studied in [22] in the context of stochastic spatio-temporal intermittency (STI). The unsuspected connections between these two problems are illustrated in the following sections.

### III. MEAN FIELD

In this section we analyze equation (6) at the mean field level. We begin by discretizing (6) on a regular  $d$ -dimensional lattice

$$\partial_t n_i = \frac{X}{2d} \sum_j (n_j - n_i) \frac{\partial V(n_i)}{\partial n_i} + n_i \nu_i; \quad (7)$$

where  $n_i = n(x_i; t)$  and the sum over  $j$  runs over the nearest neighbors of  $i$ . The Fokker-Planck equation for the one-site stationary probability  $P(n_i)$  can be easily worked-out. In mean-field approximation (i.e. substituting the values of the nearest neighbors by the average  $n$  value), the stationary Fokker-Planck equation for  $D = 1$  is

$$\frac{\partial}{\partial n} \left[ \frac{\partial V(n)}{\partial n} + (n - \ln n) P_t(n) \right] + \frac{\partial^2}{\partial n^2} n^2 P_t(n) = 0 \quad (8)$$

and its associated solution

$$P(n; \ln n) = N \frac{1}{n^2} \exp \int_0^n \frac{V^0(n) + (n - \ln n)}{n^2} dn; \quad (9)$$

where the integration constant  $N$  is determined by a normalization condition and  $\ln n$  is obtained from the self-consistency requirement

$$\ln n = \frac{\int_0^n dn n P(n; \ln n)}{\int_0^n dn P(n; \ln n)} = F(\ln n); \quad (10)$$

Let us consider two limiting cases where analytic solutions of Eq.(10) can be worked out. In the zero-dimensional case, or equivalently  $d = 0$ , the solution of (8) reads

$$P(n) = N \frac{\exp \left[ \frac{b}{p} n^p + \frac{c}{2p} n^{2p} \right]}{n^{a+2}}; \quad (11)$$

that, in terms of heights, is  $P(h) = \exp[(a+1)h - b e^{h/p} - c e^{2h/p}]$  and yields the effective potential  $V_{\text{eff}}(h) = -\ln P(h) = (a+1)h + b e^{h/p} + c e^{2h/p}$ . Clearly this coincides with the potential in (5). A complete wetting transition occurs when approaching  $a = 1$  with  $b > 0$  and critical wetting is found at  $a = 1$  with  $b = 0$ .

For spatially extended systems, in the  $d = 1$  limit, a saddle-point expansion in  $\epsilon$  yields  $V^0(n) = 0$  [17, 24]. Thus, the dynamical behavior in this limit is that of the deterministic mean-field version of (8): for any  $p > 0$ , there is a line of second order wetting transitions at  $a = 0$  and  $b > 0$ , and a line of first-order transitions at  $a > 0$  and  $b = 0$  ( $p > 2$ )  $a_c = (p+1)$ . These lines meet at a tricritical point at the origin.

For values of  $\epsilon$  other than zero or 1, the self-consistency equation  $\ln n = F(\ln n)$  has to be solved numerically. Without loss of generality, we set  $p = 2$ ,  $c = 1$ , and illustrate in Fig. 1 the three different regimes: one

stable solution at  $\ln n = 0$  (dash-dotted line); one unstable solution at  $\ln n = 0$  and a stable one at  $\ln n \neq 0$  (solid line); two stable solutions and an unstable one (dashed line). Stable solutions can be identified by a negative slope of  $F(\ln n) - \ln n$  at the intersection point [25]. A nonzero solution emerging continuously from  $\ln n = 0$  as a function of  $a$  and  $b$ , signals a second order transition. This is the case for the dash-dotted and the solid lines in the inset of Fig. 1. By contrast, when the nontrivial solution appears discontinuously as a function of  $a$  and  $b$ , the transition is first-order (dash-dotted and dashed lines). The corresponding phase diagram is depicted in Fig. 1. The solid line is a second-order phase boundary from non-wet to wet substrates. Between the two dotted lines, the wet and non-wet phases coexist as stationary solutions of the dynamical equation. The three lines join at the tricritical point at  $a = b = 0$ .

In order to determine the order parameter critical exponent in mean-field approximation, we proceed as in [13]. First, we rewrite (10) as

$$\ln n^2 = \int_0^n \frac{1}{n^2} dt \exp \left[ \frac{b}{p} t^p + \frac{t^{2p}}{2p} \right] e^{-\ln n t}; \quad (12)$$

Next, we introduce a Gaussian transformation and expand the resulting integrals for small  $\ln n$ . We end  $\ln n \sim \frac{1}{p} \ln n$ , and thus  $a_c = 0$  and  $\epsilon = 1/p$ .

### IV. BEYOND MEAN-FIELD THEORY

In this section we explore whether the mean-field phase diagram structure survives when the effects of fluctuations are taken into account. Mean-field exponents are expected to hold above the upper critical dimension  $d_c$ , which in the present case, equation (6), is known to be  $d_c = 2$ , (corresponding to 3 bulk dimensions and in the weak coupling regime of the KPZ) [11]. For positive values of  $b$  and  $d > 2$ , the second term  $n^{2p+2}$  in the effective potential is irrelevant [11] and the we are left with

$$\partial_t n = r^2 n - a n + b n^{p+1} + n; \quad (13)$$

defining the multiplicative-noise (MN) universality class [11].

We have solved (6) numerically for different system dimensions. In particular, for a one-dimensional substrate we have considered a system size  $L = 1000$ ,  $\epsilon = p = 2$ ,  $D = 1$  and  $c = 1.5$ . The time step and the mesh size were set to 0.001 and 1, respectively. We started by determining the chemical potential for which the free interface has zero average velocity. For the parameters given above we found  $a_c = 0.064$ . Then we fix  $a = a_c$  and calculate  $\ln(t) \nu$  for different values of  $b$  and large  $t$ . Length and time units are in lattice spacings and Monte Carlo steps, respectively.

### A . Critical wetting

To study critical wetting we set  $a = a_c$  and consider small values of  $b$  for which an initially pinned interface remains pinned, and increase progressively  $b$  until the non-wet phase becomes unstable at  $b_W$ . The critical point is estimated as the value  $b_W$  that maximizes the linear correlation coefficient of  $\log \langle n_i \rangle$  versus  $\log [b - b_W]$ ; the critical exponent is then determined from the corresponding slope (Fig. 2). It is found that the critical "temperature" is depressed from its mean-field value  $b_W = 0$  to  $b_W = 0.70 \pm 0.01$ , with an associated critical exponent  $\nu = 1.20 \pm 0.01$  (the error in the exponent comes from a least-squares fit). Below (above) that value we find first (second) order depinning transitions, by varying  $a$ . Therefore, as in mean-field, there is a "tricritical" point, joining a line of second order transitions ( $b > b_W$ ) with one of first order transitions ( $b < b_W$ ). The critical exponents and universality of this multiplicative-noise tricritical point has not been investigated before.

The finite coexistence region allows us to define critical wetting along a range of different paths, delimited by the dashed lines in the mean-field diagram of Fig. 1. We have checked that the value of  $\nu$  does not change when the critical point is approached along different paths within this region. Further numerical and analytical studies of this new universality class will be left for future work.

### B . Complete Wetting, $b > b_W$ case

We consider a one-dimensional substrate, with  $b = 1 > b_W$ , let the system evolve to the stationary state and then compute the order parameter  $\langle n_i \rangle$  for different values of  $a$  near its critical value. As  $a \rightarrow a_c$  a continuous transition into an absorbing state  $\langle n \rangle = 0$  is observed; it is the non-equilibrium counterpart of complete wetting. The associated critical exponent is found to be  $\nu = 1.65 \pm 0.05$  in good agreement with the prediction for the MN class,  $\nu = 1.5 \pm 0.1$  [13]. Other positive values of  $b$  yield similar results. In addition, we have simulated systems above the upper critical dimension, in  $d = 3$ , with  $L = 25$ ,  $b = 5$  and other parameters as in the one-dimensional case. Our best estimate for  $\nu$  is  $\nu = 0.96 \pm 0.05$ , indicating that this transition is governed by the weak noise fixed point of the MN class [11]. For larger values of the noise amplitude we find a strong coupling transition, in agreement with the theoretical predictions [11, 13]. Finally, we note that both numerical and renormalization group arguments lead to  $\nu = 1$  in the weak coupling regime, independently of the value of  $p$  [11]. This is at odds with the mean-field prediction  $\nu = 1/p$ . Bimer et al. [?] have recently suggested a transition from  $1/p$  to a nonuniversal behavior depending on the ratio of the noise to the strength of the spatial coupling. However, this discrepancy appears to be generic since different types of mean-field approaches yield the same (incorrect) result and the origin of the discrepancy remains unclear [13].

Since the Cole-Hopf transform of the MN equation is the same as KPZ with an additional exponential term, the MN exponents are those of KPZ if the extra term is an irrelevant term of the KPZ renormalization group flow. Note that the Cole-Hopf transform fixes the value of  $\nu = 1$  and thus the  $\nu = 0$  limit can not be considered when this transformation is used. In addition the potential  $V(h)$  is a relevant term of the EW equation. In this regime adding a non-linear potential is a relevant perturbation and it does indeed change/determine the wetting exponents (cf. with the literature on equilibrium wetting [1]). Thus EW plus a (non-linear) wetting potential is not equivalent to KPZ in the weak coupling regime plus the same wetting potential.

### C . Depinning transition at $b < b_W$

As expected, no transition is found as  $a \rightarrow a_c$  when equation (6) is solved numerically for  $b < b_W$ . Of course, the system undergoes a pinning/depinning transition when crossing the  $a_c = 0$  boundary line, but this transition is driven by the chemical potential difference rather than by the substrate potential and thus it is unrelated to wetting, where phase coexistence of the "liquid" and "gas" phases is required (i.e.  $a = a_c$ ). A very rich phenomenology associated with these transitions, have been found, however. For  $b = 4$  we find that the non-wet phase becomes unstable at  $a = 1.3$  and that the wet phase becomes unstable at  $a_c = 0.064$  (as before). Consequently, in the range  $a_c < a < a$  both phases coexist. This means that if the interface is initially close to the wall ( $n > 1$ ) it remains pinned, while if it is initially far from the wall ( $n < 1$ ) it detaches and moves away with a constant velocity. Therefore, the system undergoes a first-order transition as a function of  $a$ . In order to establish the phase boundaries we have used the following criteria. The stability of the pinned phase may be characterized by the time taken by the interface to depin in the limit  $L \rightarrow \infty$ .  $\tau_{dep}$  can be defined as the time taken by the last site of the interface to detach,  $h(x) > 0$  or  $n(x) < 1.8x$ . Similarly, we may define  $\tau_{det}$  as the time characterizing the asymptotic exponential decay of  $\langle \ln(t) \rangle$ , where the angular brackets denote averages of independent runs (typically  $10^5 - 10^6$  in our simulations). We have verified that both definitions yield analogous results. As shown in Fig. 3A, for  $a > a_c$ ,  $\tau_{det}$  saturates with increasing system size and thus the interface detaches in a finite time. Within the coexistence region we have found two different regimes: close to the stability threshold of the pinned phase there is a narrow stripe  $1.22 < a < 1.3$  where the detaching time grows approximately as a power-law. For  $a_c < a < 1.22$   $\tau_{det}$  grows exponentially with  $L$ . In both cases  $\tau_{det} \rightarrow \infty$  as  $L \rightarrow \infty$ , implying that the pinned phase is stable in the thermodynamic limit. Due to the very large characteristic times, we cannot discard the possibility that the power-laws are also (asymptotically) exponentials. The

study of the asymptotic behavior of the detaching times requires longer simulations, beyond our current computer capabilities. Finally, the non-monotonic behavior of the characteristic times, as well as the step in the curve for  $a = 1.28$ , may be accounted for by the presence of two different competing mechanisms as described in [10]: once a site is detached it pulls out its neighbors which, in turn, pull out their neighbors in a cascade effect until the whole interface is depinned in a time which grows linearly with  $L$ . This is more likely for small systems, but the probability that a site gets detached increases with the system size.

Another way to characterize the power-law regime is to analyze the single-site stationary probability density function (ss-pdf), defined as the average of  $n(t)$  over pinned states rather than over all runs. Figure 3 shows the unnormalized ss-pdf for different values of  $a$ . In the exponential regime ( $a < 1.22$ ) the histogram exhibits a maximum at a pinned state with  $h_{ni} > 0$ . In the power-law regime, however, the histogram develops a secondary maximum near  $n = 0$ , indicating that a fraction of the interface depins. As  $a$  increases, the secondary maximum, at zero  $n$ , increases while the maximum, at finite  $n$ , decreases. At the stability edge ( $a = 1.3$ ) the histogram changes abruptly into a delta function at  $n = 0$  and the pinned phase becomes unstable.

The differences between the exponential and power-law regimes are also observed in a space-time snapshot of a numerical solution of (6). In Fig. 4 we plot the stationary field  $n$ , for  $a = 1.28$ , exhibiting patterns characteristic of STI [22]. The main feature of these patterns is the appearance of depinned patches (absent for values of  $a$  in the exponential regime) with a wide range of sizes and life-times within the pinned phase. This regime, overlooked in previous studies of nonequilibrium depinning transitions [17, 18], seems to correspond to the power-law regime described earlier. It is therefore restricted to a narrow range between the exponential and the depinned regimes. This finding is at odds with results of previous work claiming that STI is generic in the coexistence region [22].

A typical profile in terms of  $h$  is shown in Fig. 5. The depinned interfacial regions form triangles with constant average slopes. These triangular droplets are similar to those described in the discrete model of [18]. By taking averages of (5), the typical slope  $s$ , of the triangular facets is determined through

$$j_R \beta^2 = a + 1; \quad (14)$$

where  $j_R$  is the renormalized non-linear coefficient of the KPZ equation. In order to verify equation (14) we have fixed  $\nu = p = D = 1$ ,  $\alpha = 1$  and  $a = 2.16$ . Averaging over 250,000 different triangles, we find an average slope  $s = 1.781$ , while the value of  $j_R$  calculated from the tilt-dependent velocity of the depinned interface [8] yields  $j_R = 0.9934$  from which  $s = 1.784$ , in excellent agreement with the previously measured value.

We also studied the size distribution of triangles within

the power-law regime. Our results correspond to  $\nu = p = D = 1$ ,  $\alpha = 1$ ,  $L = 500$ ,  $b = 4$ , and the following values of  $a$ : 2.12; 2.14; 2.15, and 2.16, and are summarized in Fig. 6.  $a = 2.10$  is the boundary between the power-law and exponential regimes and the pinned phase is unstable for  $a > 2.18$ . The maximum size of the depinned regions increases as this instability is approached. Our data suggests an exponential dependence on the size of the triangular base. This indicates that there is a maximum size for the depinned regions and thus rigorous scale invariance (typical of growth driven by a coarsening mechanism) of the STI region is ruled out. More explicitly, the distribution of triangle sizes,  $l$ , is described very well by the function  $\exp[-3.44(a - 2.176)l]$ , implying that the exponential slopes in Fig. 6 are proportional to  $a - a_c$ . Clearly, triangles with a base less than  $2/3$  cannot be visualized due to the discretization of equation (6). A simple extrapolation indicates that the triangles become imperceptibly small for  $a = 2.05$ , in good agreement with the value obtained for the boundary between the power-law and exponential regimes. Therefore, we cannot rule out the possibility that the triangles are ubiquitous throughout the coexistence region (although not always visible in a discrete numerical simulation) in which case the power-law detaching times should turn into exponentials for large enough times and system sizes. In this case the force exerted by the non-linear KPZ term on the triangular facets against the direction of growth, at late times, guarantees the stability of the pinned phase [18] throughout the finite coexistence region.

Finally, we study the phase-coexistence regime in a two-dimensional system to check whether the triangular patterns survive in higher dimensionalities. In particular, we consider a system size  $100 \times 100$  and take  $a = 2$ ,  $b = 4$ , well within the coexistence region. We find structures as those shown in Fig. 7: the triangles become pyramids. Note that the edges of the pyramid bases are parallel to the axes of the discretization-lattice. This suggests that the pyramids are lattice artefacts and that a continuum system may exhibit conical structures.

## V. CONCLUSIONS

We have investigated a continuum model for nonequilibrium wetting transitions. The model consists of a KPZ equation in the presence of a short-ranged substrate potential, and is the most natural non-equilibrium extension of the interface displacement models used in equilibrium wetting. It can be mapped into a multiplicative noise problem, enabling simple theoretical calculations at the mean-field level. Numerical simulations reproduce a phase diagram analogous to that obtained within mean-field, including first as well as second-order phase transitions. In particular, we have found complete wetting and critical wetting transitions, as well as a finite area in the temperature-chemical potential phase diagram where pinned and depinned phases coexist. This finite coexis-

tence region allows us to define critical wetting along a range of paths that are, however, characterized by the same critical exponents. Within this area we identified two regimes. In the first, the lifetime of the pinned phase grows exponentially with increasing system size and its ss-pdf is bell-shaped. The second one exhibits ST I, lifetimes consistent with a power-law, and a double-peaked ss-pdf. The main feature of the latter regime is the presence of triangular structures that have been characterized by their slopes and size distributions.

An interesting open problem is that of the equilibrium limit of non-equilibrium wetting. The Cole-Hopf transform precludes the limit  $\epsilon = 0$  to be studied using this method. Moreover, we have noted how the behavior of the EW equation in the presence of a wetting potential differs from the weak-noise regime of the MN equation. This leaves the crossover to equilibrium wetting an open challenge. In addition, the effects of long-ranged potentials on the phenomenology described here remain to be

investigated.

Finally it would be extremely interesting to develop experiments in order to explore the rich, non-equilibrium phenomenology described in the previous sections; liquid-crystals are in our opinion good candidates for this. It is our hope that this work will stimulate experimental studies in this direction.

## V I. ACKNOWLEDGMENTS

We acknowledge financial support from the E.J. through Contracts No. ERBFMRXCT980171 and ERBFMRXCT980183, by the Ministerio de Ciencia y Tecnología (FEDER) under project BFM 2001-2841 and from the Fundação para a Ciência e a Tecnologia, contract SFRH/BPD/5654/2001.

- 
- [1] S. Dietrich, in *Phase Transitions and Critical Phenomena*, vol. 12, edited by C. Domb and J. Lebowitz, Academic Press (1983); D.E. Sullivan and M.M. Teb da Gama, in *Fluid Interfacial Phenomena*, ed. C.A. Coxton. Wiley, New York (1986).
- [2] M.E. Fisher, in *Jerusalem Winter School for Theoretical Physics: Statistical Mechanics of Membranes and Surfaces*, vol. 5, edited by D. Nelson, T. Piran and S. Weinberg, World Scientific (1989).
- [3] E. Brezin, B.I. Halperin, and S. Leibler, *J. Phys. (Paris)* 44, 775 (1983).
- [4] The derivation of this functional is far from trivial. Ideally one should constrain the interface, away from its equilibrium position, in the configuration  $h(x)$  and using the microscopic Hamiltonian, take a partial trace over the bulk variables. Note also that the displacement model assumes the existence of an interface and thus is only valid below the bulk critical temperature, where distinct "liquid" and "gas" phases are defined.
- [5] If, instead, one considers long-range (van der Waals) interactions, the potential has the general form [1].
- $$V(h) = b(T)h^{-m} + ch^{-n}; \quad n > m > 0: \quad (15)$$
- [6] R. Lipowsky, *J. Phys. A* 18, L585 (1985).
- [7] S.F. Edwards and D.R. Wilkinson, *Proc. R. Soc. London A* 381, 17 (1982).
- [8] A.-L. Barabasi and H.E. Stanley, *Fractal Concepts in Surface Growth*, Cambridge University Press, Cambridge 1995.
- [9] H.H. Inrichsen, R. Livi, D. Mukamel, and A. Politi, *Phys. Rev. Lett.* 79, 2710 (1997).
- [10] F. de los Santos, M.M. Teb da Gama, and M.A. Muroz, *Europhys. Lett.* 57, 803 (2002).
- [11] G. Grynstein, M.A. Muroz, and Y. Tu *Phys. Rev. Lett.* 76, 4376 (1996). Y. Tu, G. Grynstein and M.A. Muroz, *Phys. Rev. Lett.* 78, 274 (1997). M.A. Muroz and T. Hwa, *Europhys. Lett.* 41, 147 (1998).
- [12] T. Bimer, K. Lippert, R. Muller, A. Kune, and U. Behn, *Phys. Rev. E* 65, 046110 (2002).
- [13] W. Genovese and M.A. Muroz, *Phys. Rev. E* 60, 69 (1999).
- [14] See, P. Le Doussal and K.J. Wiese, *Condmat/0208204*; and references therein.
- [15] J. Villain, *J. Phys. I*, 19, 1 (1991); A. Pinelli and J. Villain, *The Physics of Crystal Growth*, Cambridge University Press, New York, 1998.
- [16] R. Muller, K. Lippert, A. Kune, and U. Behn, *Phys. Rev. E* 56, 2658 (1997).
- [17] L. Giada and M. Marsili, *Phys. Rev. E* 62, 6015 (2000).
- [18] H.H. Inrichsen, R. Livi, D. Mukamel, and A. Politi, *Phys. Rev. E* 61, R1032 (2000).
- [19] J. Krug and P. Meakin, *J. Phys. A* 23, L987 (1990).
- [20] The influence of the sign of  $\epsilon$  has been previously investigated in [9, 11, 18].
- [21] The equivalence of equations (5) and (6) is reminiscent of a result in equilibrium wetting establishing that at the mean-field level (dropping the noise and ignoring spatial variations of the order parameter) critical wetting in systems with long-range forces is equivalent to complete wetting in systems with short-range interactions; R. Lipowsky, *Phys. Rev. Lett.* 52, 1429 (1984).
- [22] M.G. Zimmermann, R. Toral, O. Piro, and M. San Miguel, *Phys. Rev. Lett.* 85, 3612 (2000).
- [23] N.G. van Kampen, *Stochastic Processes in Physics and Chemistry*, North Holland (1992).
- [24] C. van der Broeck, J.M.R. Parrondo, J. Amaro, and A. Hernandez-Machado, *Phys. Rev. E* 49, 2639 (1994).
- [25] M. Shiino, *Phys. Rev. A* 36, 2393 (1987).

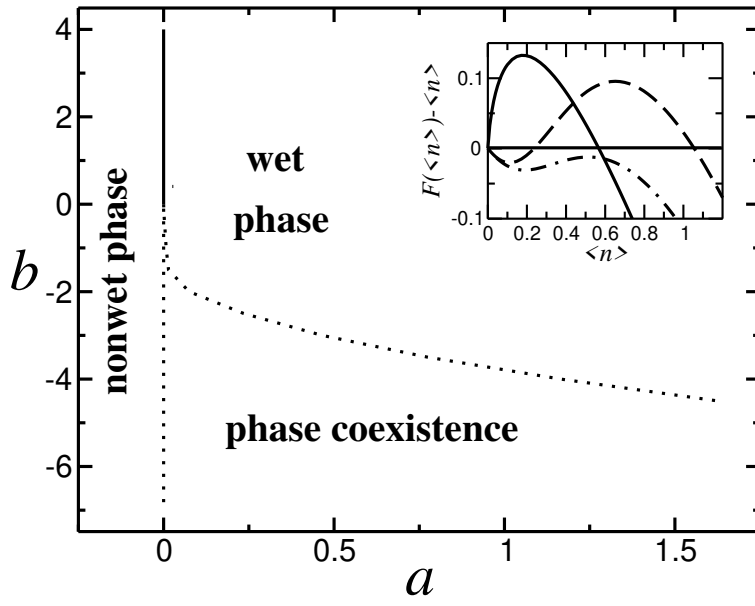


FIG. 1: Mean-field phase diagram and typical solutions of the equation  $F(\langle n \rangle) = h\langle n \rangle$  (temperature in units such that  $k_B = 1$ ).

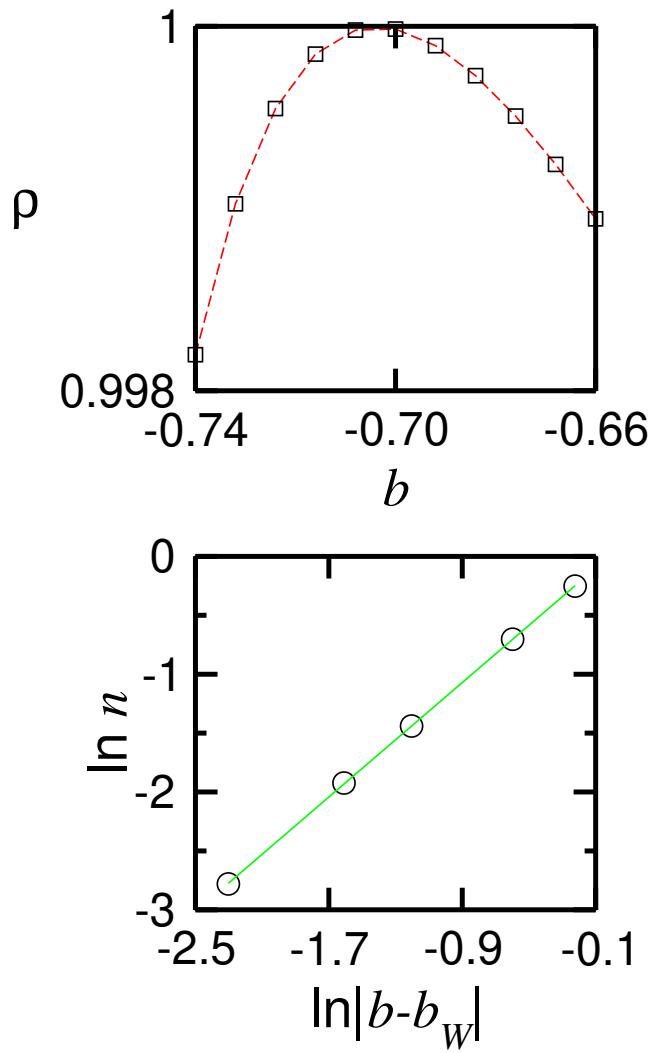


FIG. 2: Top: linear correlation coefficient for  $\ln n$  as function of  $\ln|b - b_w|$  for different values of  $b_w$ . The maximum gives the best estimate of  $b_w = -0.70 \pm 0.01$ . Bottom: log-log plot of  $\ln n$  as function of  $\ln|b - b_w|$  in the vicinity of the critical point. The line is a least-squares fit; from its slope the critical wetting exponent is found to be  $1.20 \pm 0.02$ .

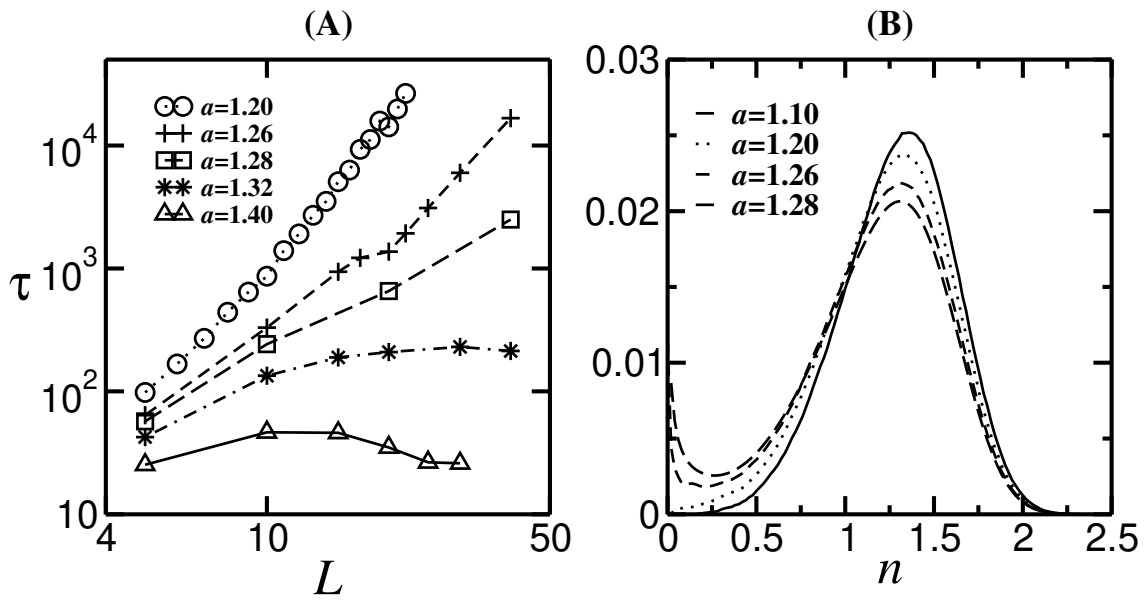


FIG. 3: (A) Characteristic depinning times and (B) ss-pdf for various representative values of  $a$ .

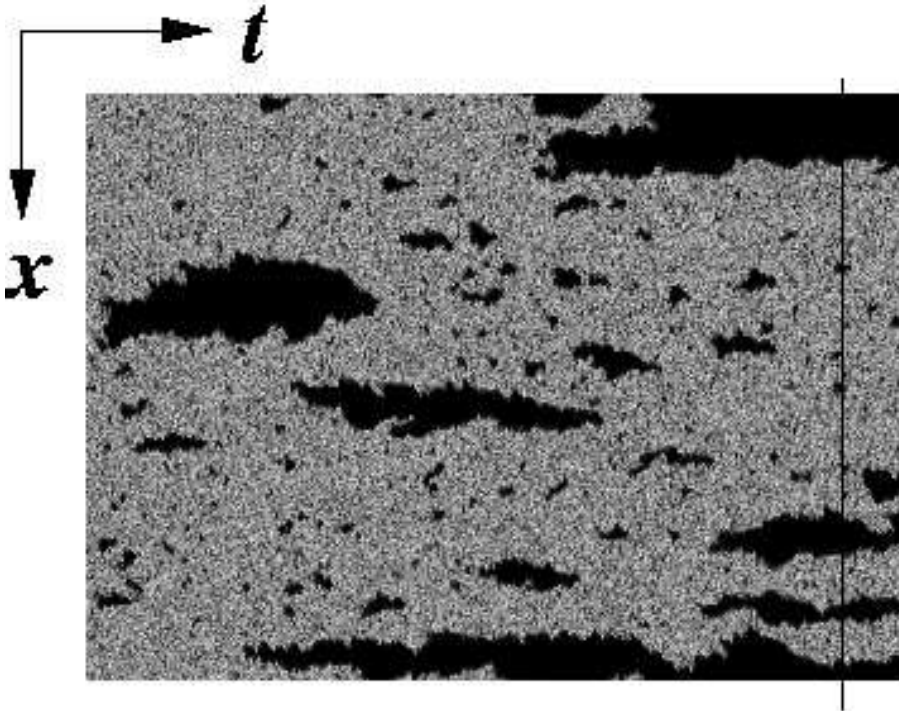


FIG. 4: Configuration in the  $n$ -representation for  $a = 1.18$  and  $b = 4$ . Depinned regions ( $n < 1$ ) are colored in dark-grey and pinned ones ( $n > 1$ ) in light-gray. 1000 time slices are depicted at intervals of 50 time units. The system size is  $L = 500$ .

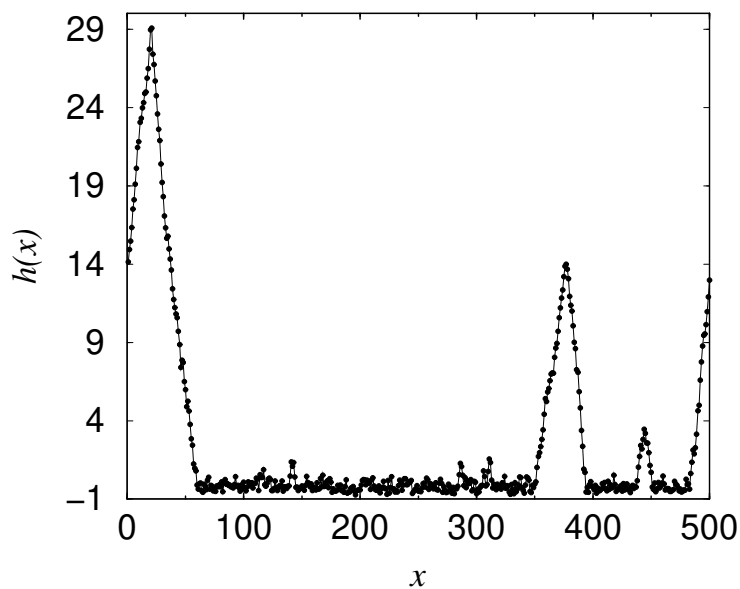


FIG. 5: Instantaneous configuration of the interface for time slice 400 (marked with a line in Fig. 4). Parameters as in Fig.

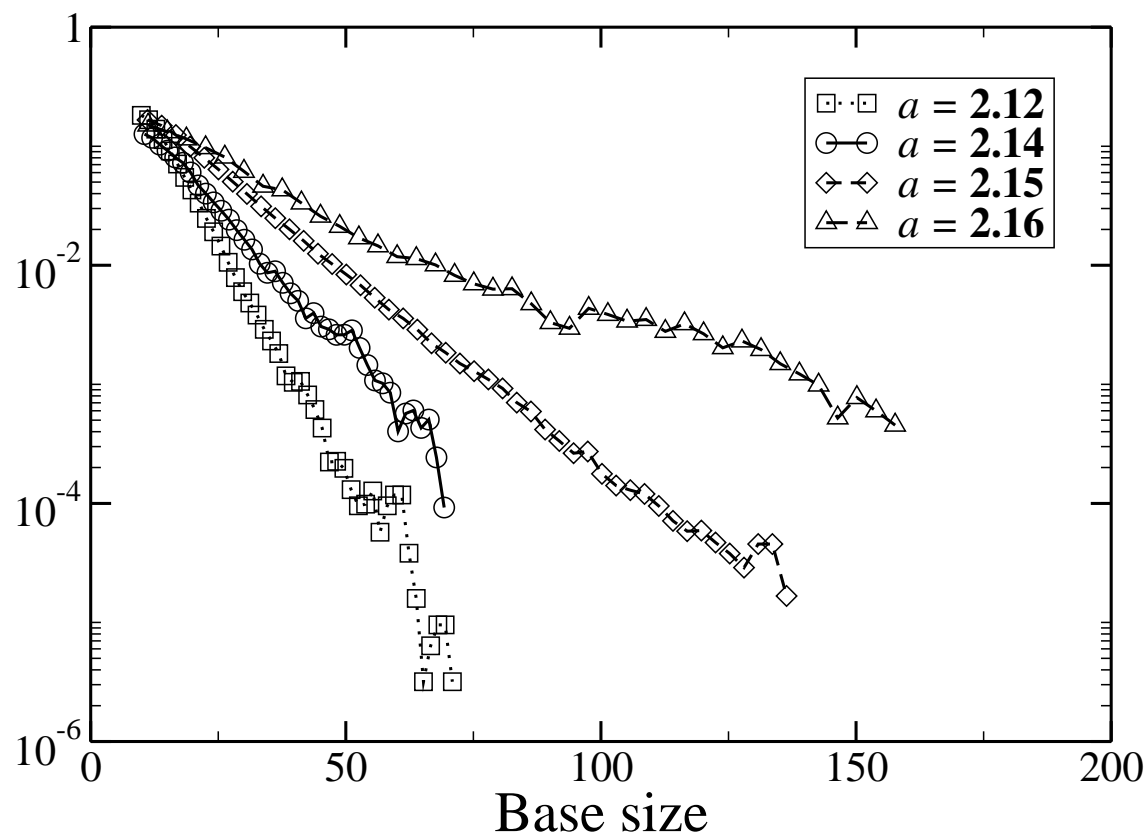


FIG. 6: Distribution of triangles as a function of the size of the triangular base, for  $a = 2.12; 2.14; 2.15$  and  $2.16$ .

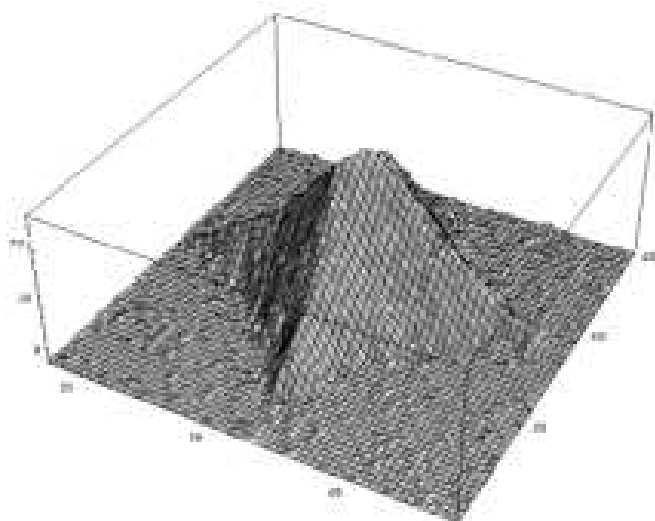
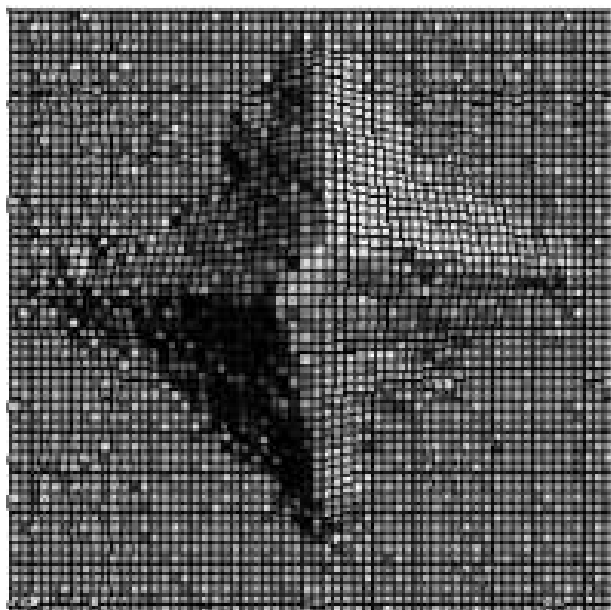


FIG .7: Snapshot of an interface con guration for a  $100 \times 100$  system (not all the substrate is show n) and param eters  $a = 2$  and  $b = 4$ .